Hybrid synthesis of scalar wave envelopes in two-dimensional random media having rich short-wavelength spectra

Haruo Sato
Department of Geophysics, Tohoku University, Sendai, Japan

Mike Fehler
Los Alamos National Laboratory, Los Alamos, New Mexico, USA

Tatsuhiko Saito
Department of Geophysics, Tohoku University, Sendai, Japan

Received 5 July 2003; revised 12 February 2004; accepted 23 February 2004; published 16 June 2004.

[1] Wave trains in high-frequency seismograms of local earthquakes are mostly composed of incoherent waves that are scattered by distributed heterogeneities within the lithosphere. Their phase variations are very complex; however, their wave envelopes are systematic, frequency-dependent, and vary regionally. Stochastic approaches are superior to deterministic wave-theoretical approaches for modeling wave envelopes in random media. The time width of a wavelet is broadened with increasing travel distance mostly because of diffraction caused by the long-wavelength components of random velocity inhomogeneity. The Markov approximation for the parabolic wave equation is effective for the synthesis of envelopes for random media whose spectra are poor in short-wavelength components; however, we have to consider the contribution of large-angle nonisotropic scattering if the random media are rich in short-wavelength inhomogeneities. Multiple nonisotropic scattering can be reliably modeled as isotropic scattering by using an effective isotropic scattering coefficient given by the momentum transfer scattering coefficient, which is a reciprocal of the transport mean free path. It is mostly controlled by the short-wavelength spectra of random media. We propose a hybrid method for the synthesis of whole wave envelopes that uses the envelope derived from the Markov approximation as a propagator in the radiative transfer integral equation for isotropic scattering. The envelopes resulting from the hybrid method agree well with ensemble average envelopes calculated by averaging envelopes from individual finite difference simulations of the wave equation for a suite of random media. *INDEX TERMS:* 0902 Exploration Geophysics: Computational methods, seismic; 7203 Seismology: Body wave propagation; 7218 Seismology: Lithosphere and upper mantle; 7260 Seismology: Theory and modeling; *KEYWORDS:* envelope, scattering, random media, radiative transfer theory, stochastic approach

Citation: Sato, H., M. Fehler, and T. Saito (2004), Hybrid synthesis of scalar wave envelopes in two-dimensional random media having rich short-wavelength spectra, *J. Geophys. Res.*, *109*, B06303, doi:10.1029/2003JB002673.

1. Introduction

[2] Seismic waves radiated with a very short duration time from a microearthquake source are scattered by distributed random heterogeneities in the lithosphere and undergo amplitude decay and envelope broadening as illustrated in Figure 1. Observational and theoretical studies of this envelope collapsing phenomenon have led to methods for measuring medium heterogeneity and the earthquake source process [*Aki*, 1980; *Atkinson*, 1993]. Models of scattering by random inhomogeneity predict that the frequency dependence of scattering loss is related to the spectra of random media. A comprehensive review of attenuation and scattering in the earth is given by *Sato et al.* [2002]. Most studies about attenuation in the earth have focused on direct wave amplitudes; however, we have proposed that the amplitude decay of the direct arrival with increasing travel distance and the excitation of coda waves that follow the direct arrivals should be simultaneously explained by a unified model. *Sato* [1984] proposed a model for amplitude attenuation and envelope formation of three-component seismograms in random elastic media. His model is based on the single scattering approximation of the radiative transfer theory with the Born approximation for polarized elastic waves. Sato noted that forward scattering by long-wavelength components of velocity inhomogeneity lead to travel time fluctuations but do not remove energy from a propagating wave field. Thus, for the calculation of scattering loss during propagation, he ignored forward scattering and summed up

0148-0227/04/2003JB002673$09.00

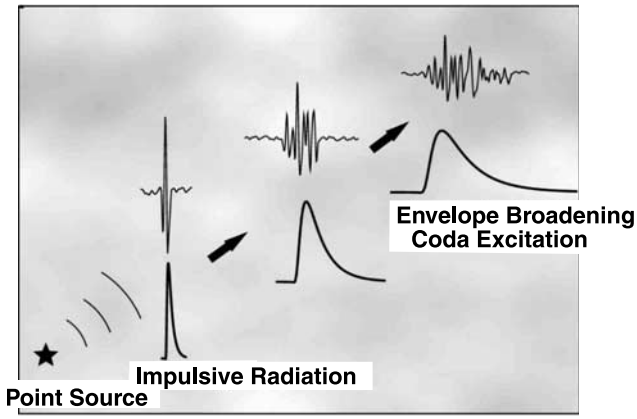

Figure 1. Schematic illustration of wave propagation in a random medium. A wavelet impulsively radiated from a point source decays with increasing travel distance. Envelopes represent the modulation effect due to scattering.

waves scattered at large angles by short-wavelength components, which form the coda wave envelope.

[3] While forward scattering does not remove energy from a propagating wave field, it is very important to consider forward scattering and/or diffraction when modeling complex envelopes around direct arrivals. Focusing on the diffraction due to long-wavelength components of velocity inhomogeneity, *Sato* [1989] and *Scherbaum and Sato* [1991] explained the broadening of *S* wave envelopes of microearthquakes with increasing travel distance observed in Kanto, Japan, by using a model based on the Markov approximation for the parabolic wave equation for scalar waves in random media [*Lee and Jokipii*, 1975]. This approximation is valid when the wavelength is smaller than the characteristic scale of medium inhomogeneity. *Fehler et al.* [2000] confirmed that the envelope that is directly simulated by the Markov approximation is in agreement with the statistical average envelope of waves that are synthesized numerically by using the finite difference (FD) method. We will call the former and the latter the Markov envelope and the FD envelope, respectively. *Fehler et al.* [2000] used Gaussian spectra for characterizing random media because they allowed us to easily deal with the mathematically tractable problem of modeling envelope formation. Envelope broadening in media with Gaussian spectra is frequency-independent; however, observed envelopes vary with frequency. *Obara and Sato* [1995] reported that the S-wave envelope broadening for frequencies higher than 3 Hz in the back arc side of the volcanic front is larger that that in the forearc side in Kanto-Tokai, Japan. Beneath this area, the Pacific plate is subducting. The regional difference in envelope broadening might reflect the regional difference in the spectra of lithospheric inhomogeneity. In the laboratory, *Fukushima et al.* [2003] measured the collapse of the envelope of ultrasonic shear waves propagating through different kinds of rock samples by using a laser Doppler vibrometer. They reported that the envelope broadening in Oshima granite is much larger than in Tamura gabbro at 1 MHz. They suggested the importance to envelope broadening of large-angle scattering by small-scale random heterogeneities and cracks in addition to diffraction effects due to large-scale inhomogeneities.

[4] Recently, extending *Shishov*'s work [1974] on three-dimensional (3-D) random media having Gaussian spectra, *Saito et al.* [2002] succeeded in formulating the envelope synthesis of spherically outgoing waves radiated from a point source in 3-D random media of von Kármán–type, which are more appropriate to describe the inhomogeneities of the real earth having a power law spectra [e.g., *Shiomi et al.*, 1997]. In a following paper [*Saito et al.*, 2003], we compared Markov envelopes with FD envelopes in 2-D von Kármán–type random media. The comparison is generally good for a small time window containing the peak arrival. The fit is good from the onset to coda in random media with weak short-wavelength spectra; however, Markov envelopes are smaller than FD envelopes at a large lapse time in random media with rich short-wavelength spectra since the large-angle scattering contribution is not reliably modeled in the Markov approximation. To extend the Markov approximation approach for envelope synthesis around the peak arrival, *Saito et al.* [2003] proposed a partial addition of scattered wave power by using the conventional radiative transfer equation for the isotropic scattering process in order to explain the coda excitation. They used the fact that the scattering process is well represented by isotropic scattering when multiple scattering dominates, where the effective isotropic scattering coefficient is given by the momentum transfer scattering coefficient [see *Morse and Feshbach*, 1953]. Their model succeeded in explaining the whole envelope of scalar waves radiated from a point source in 2-D von Kármán–type random media; however, their model has a defect that the propagator used in the radiative transfer equation is a delta function and it does not contain the diffraction effect due to long-wavelength spectra of random media.

[5] We note that *Kravstov* [1992] developed a model for describing the scattering of waves by small inhomogeneities in the background of large-scale inhomogeneities as an extension of the distorted-wave Born approximation used in the quantum theory. Here we propose a hybrid method to synthesize the whole envelope of scalar waves radiated from a point source from the onset to coda. We focus on the case of 2-D random media especially having rich short-wavelength spectra. The basic idea is to use the Markov envelope as a propagator in the radiative transfer integral equation for isotropic scattering. The propagator includes the diffraction effect due to long-wavelength spectra and, in addition, isotropic scattering reliably models the contribution of short-wavelength spectra.

[6] First, we briefly describe the mathematical basics for the statistical study of wave propagation in random media and the derivation of Markov envelopes, and then we show comparisons of Markov envelopes with FD envelopes. Second, we propose a hybrid method for the whole envelope synthesis on the basis of the radiative transfer theory, and then we compare the simulated envelopes with FD envelopes. Finally, we discuss possible future developments.

2. FD Envelopes and Markov Envelopes in Random Media

2.1. von Kármán–Type Random Media

[7] For the study of stochastic wave propagation through 2-D inhomogeneous media, we imagine an ensemble of

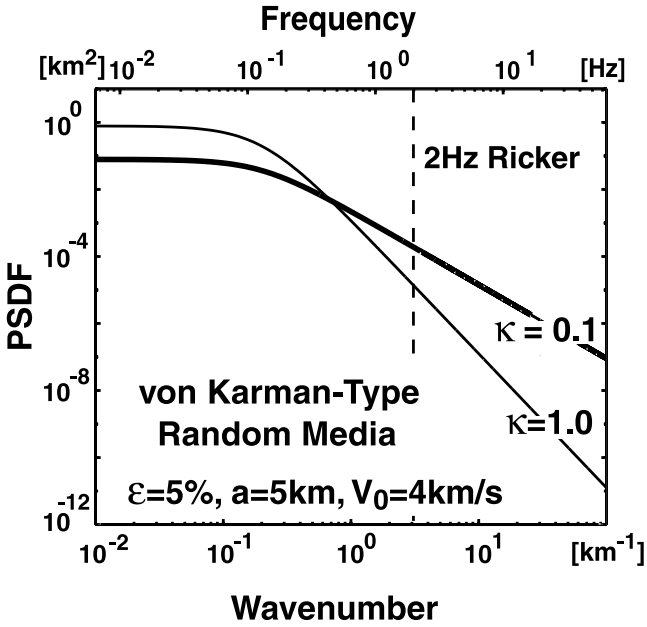

Figure 2. Power spectral density functions (PSDFs) of two-dimensional (2-D) von Kármán–type random media used in this study.

random media. In each medium, the wave-velocity inhomogeneity is written as $V(\mathbf{x}) = V_0\{1 + \xi(\mathbf{x})\}$, where V_0 is the average wave velocity and fractional velocity fluctuation $\xi(\mathbf{x})$ is a random function of space coordinate $\mathbf{x}$. The ensemble of random media is mathematically given by a set of random functions $\{\xi(\mathbf{x})\}$, where $\langle\xi(\mathbf{x})\rangle = 0$. The angular brackets mean the ensemble average. We assume that the randomness is statistically homogeneous and isotropic. The random media can be characterized by the auto-correlation function (ACF) of fractional velocity fluctuation $R(\mathbf{x}) \equiv \langle\xi(\mathbf{x} + \mathbf{x}')\xi(\mathbf{x}')\rangle$. The magnitude of inhomogeneity is given by the mean square (MS) fractional fluctuation $\varepsilon^2 \equiv R(0) = \langle\xi(\mathbf{x})^2\rangle$, and the characteristic scale is given by the correlation distance a. The power spectral density function (PSDF) is given by the Fourier transform of the ACF, $P(\mathbf{m}) = \int\int_{-\infty}^{\infty} R(\mathbf{x})e^{-i\mathbf{m}\mathbf{x}}d\mathbf{x}$, where argument $\mathbf{m}$ is the wave number vector.

[8] Well log data and seismic studies suggest that the PSDF of fractional fluctuation of seismic velocity obeys a power law in wave number [e.g., *Wu and Aki*, 1985; *Shiomi et al.*, 1997; *Goff and Holliger*, 1999]. The most typical random media having power law spectra as asymptote are von Kármán–type, which were first introduced for the study of turbulent in fluids [*Tatarskii*, 1971]. In 2-D, the von Kármán–type PSDF of order κ is given by

$$P(\mathbf{m}) = P(m) = \frac{4\pi\varepsilon^2 a^2\kappa}{(1 + a^2m^2)^{\kappa+1}} \propto m^{-2\kappa-2} \quad \text{for} \quad am \gg 1, \tag{1}$$

where wave number $m = |\mathbf{m}|$. The PSDF obeys a power law for large wave numbers and the exponent is $-2\kappa - 2$, which means that short-wavelength components in the spectra increase with decreasing order κ. The corresponding ACF is written by

$$R(\mathbf{y}) = R(y) = \frac{\varepsilon^2 2^{1-\kappa}}{\Gamma(\kappa)}\left(\frac{y}{a}\right)^{\kappa} K_{\kappa}\left(\frac{y}{a}\right), \tag{2}$$

where $y = |\mathbf{y}|$, Γ is a Gamma function, and K_κ is the modified Bessel function of the second kind.

[9] As an example, PSDFs for $\kappa = 0.1$ and 1.0 are shown in Figure 2. We take $\kappa = 1.0$ to represent random media with poor short-wavelength spectra. We choose $\kappa = 0.1$ for a typical example of random media with rich short-wavelength spectra. Note that $K_0(y)$ for $\kappa = 0$ diverges as $y \to 0$.

2.2. FD Envelopes

[10] We numerically simulate wave propagation through 50 realizations of 2-D von Kármán–type random media having $V_0 = 4$ km/s, $\varepsilon = 5\%$, $a = 5$ km, for each case of $\kappa = 0.1$ and $\kappa = 1.0$. The dimension of each medium is 205 km by 300 km. We use a finite difference solution of the acoustic wave equation to numerically simulate the wave field from a 2 Hz Ricker wavelet isotropic point source in each random medium realization. Finite difference modeling is accomplished with a 2-D FD code that has fourth-order accuracy in space and second-order accuracy in time. The code uses *Holberg* [1987] coefficients, which are optimal for minimizing grid dispersion for a given number of grid points per wavelength. We use Higdon absorbing boundaries [*Higdon*, 1991]. We use a grid spacing of 50 m and a time step of 4 ms. Waveforms are simulated at receivers with 25 km spacing at distances of 0 to 200 km from the source. In our model, there is 50 km between the source location and the nearest boundary of the model and 50 km between the most distant receiver and the nearest model boundary. Boundary reflections from the near-source and near-receiver regions should not arrive until 25 s after the direct arrival in the background medium. A detailed description of the FD simulation is given by *Fehler et al.* [2000]. Figures 3a and 3b show examples of FD simulations for $\kappa = 0.1$ and $\kappa = 1.0$, where the abscissa is reduced time by travel time calculated by background velocity V_0. Broadening of a pulse, travel time fluctuation and excitation of scattered waves are clearly seen in these FD wave traces. Travel time fluctuation for the case of $\kappa = 1.0$ is larger than that for the case of $\kappa = 0.1$ because of the difference in long-wavelength spectra. Excitation of scattered waves for the case of $\kappa = 0.1$ is larger than that for the case of $\kappa = 1.0$ because of the difference in short-wavelength spectra.

[11] Smoothing the average of 50 squared wave traces over a 0.32 s window at each receiver, we obtain the MS envelope. Taking the square root of MS envelope, we get the root-mean-square (RMS) envelope at each receiver. We call them FD envelopes. Shaded curves in Figures 4a and 4b show the temporal changes in FD envelopes at eight receivers in von Kármán–type random media of $\kappa = 0.1$ and $\kappa = 1.0$, respectively. The maximum peak amplitude of the envelope decreases and the time width broadens with increasing travel distance. The excitation of coda waves in media with $\kappa = 0.1$ is larger than that in media with $\kappa = 1.0$

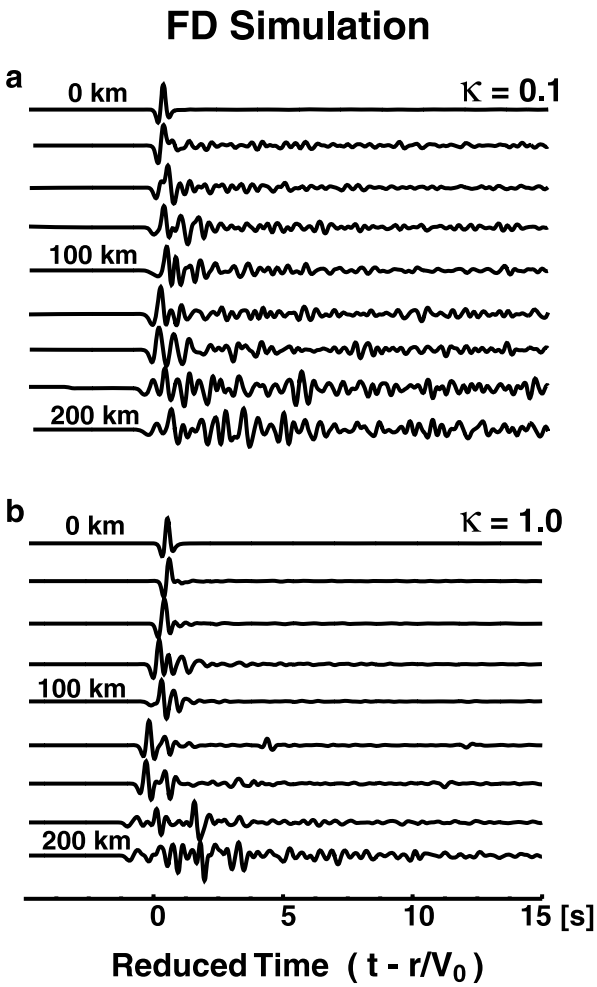

Figure 3. Variation of wave traces with travel distance for a 2 Hz Ricker wavelet source radiation in von Kármán–type random media by using the finite difference (FD) method, where numerals are distances from the point source and amplitude is normalized by the peak value in each trace: (a) $\kappa = 0.1$ and (b) $\kappa = 1.0$.

as shown by the long envelope tails after the large initial peaks for the case of $\kappa = 0.1$.

2.3. Markov Envelopes

2.3.1. Parabolic Wave Equation

[12] When the fractional velocity fluctuation is small, $|\xi(\mathbf{x})| \ll 1$, the wave equation for scalar waves $u(\mathbf{x}, t)$ is written as

$$\left(\Delta - \frac{1}{V_0^2}\frac{\partial^2}{\partial t^2}\right)u(\mathbf{x},t) + \frac{2}{V_0^2}\xi(\mathbf{x})\frac{\partial^2}{\partial t^2}u(\mathbf{x},t) = 0. \tag{3}$$

For the study of cylindrically outgoing waves radiated from a point source, we take the source at the origin of a polar coordinate system, where $r = |\mathbf{x}|$ and angle θ is measured from the direction toward a receiver from the source. Scalar waves are written as a superposition of harmonic cylindrical waves of amplitude U at angular frequency ω as

$$u(\mathbf{x},t) = \frac{1}{2\pi}\int_{-\infty}^{\infty}\frac{U(r,\theta,\omega)}{\sqrt{r}}e^{i(kr-\omega t)}d\omega, \tag{4}$$

where wave number $k = \omega/V_0$. If we model the scattering contribution of long-wavelength spectra, we may use the parabolic approximation for the wave equation. Substituting equation (4) into equation (3) and neglecting the second derivative with respect to r, we obtain the parabolic wave equation:

$$2ik\frac{\partial}{\partial r}U(r,\theta,\omega) + \frac{1}{r^2}\frac{\partial^2}{\partial\theta^2}U(r,\theta,\omega) - 2k^2\xi(r,\theta)\,U(r,\theta,\omega) = 0. \tag{5}$$

Liu and Wu [1994] and *Saito et al.* [2003] reported that it is enough to consider forward scattering and diffractions around the global ray direction when we focus on waves around direct arrivals. We note that the parabolic approximation is used under the condition that the wave number is much larger than the reciprocal of correlation distance $k \gg 1/a$.

2.3.2. Markov Approximation for Quasi-Monochromatic Waves

[13] In order to derive the temporal change in wave envelopes in random media we define the two-frequency mutual coherence function (TMCF) on a transverse axis at a distance r from the source [e.g., *Ishimaru*, 1978]. It means the correlation of the wave field between different locations θ_1 and θ_2 and different angular frequencies ω_1 and ω_2,

$$\Gamma_2(\theta_1,\theta_2,r,\omega_1,\omega_2) \equiv \langle U(r,\theta_1,\omega_1)\,U^*(r,\theta_2,\omega_2)\rangle, \tag{6}$$

where the asterisk means complex conjugate. The following procedure is along the line given by *Fehler et al.* [2000] and *Saito et al.* [2003]. Since the random media are statistically homogeneous, Γ_2 depends on the difference angle $\theta_d \equiv \theta_1 - \theta_2$ only. For quasi-monochromatic waves, that is, $\omega_1 \approx \omega_2$, the master equation for Γ_2 is written as

$$\frac{\partial}{\partial r}\Gamma_2 + i\frac{k_d}{2k_c^2}\frac{1}{r^2}\frac{\partial^2}{\partial\theta_d^2}\Gamma_2 + k_c^2[A(0) - A(r\theta_d)]\Gamma_2 + \frac{k_d^2}{2}A(0)\Gamma_2 = 0, \tag{7}$$

where the center of mass and difference coordinates in the wave number space are $k_c = (k_1 + k_2)/2$ and $k_d = k_1 - k_2$

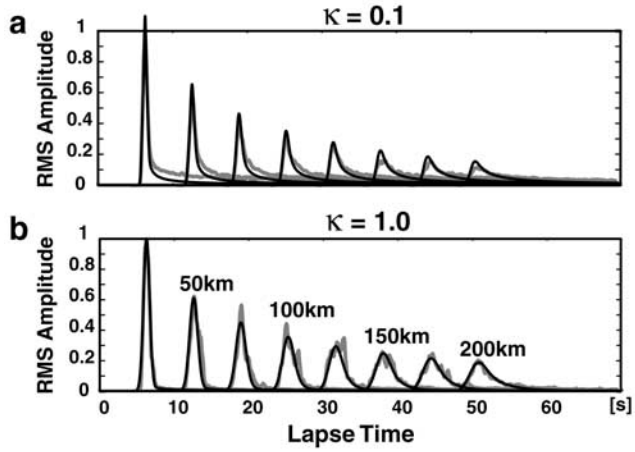

Figure 4. FD envelopes (shaded) and Markov envelopes (solid) for a 2 Hz Ricker wavelet source radiation in 2-D von Kármán–type random media, where numerals are distances from the point source: (a) $\kappa = 0.1$ and (b) $\kappa = 1.0$.

($k_d \ll k_c$), respectively. Corresponding coordinates for angular frequency will also be used. The above derivation is called the Markov approximation [*Tatarskii*, 1971]. Note that this approximation accounts only for strong forward scattering and diffraction effects; no back scattering is considered.

[14] The contribution of inhomogeneity is given by the longitudinal integral of the ACF,

$$A(r\theta_d) = \int_{-\infty}^{\infty} dz R(r\theta_d, z), \tag{8}$$

where the z axis is chosen to be the radial direction and $r\theta_d$ is a distance on the transverse axis at a distance r from the source. For von Kármán–type random media, the longitudinal integral A is directly calculated from the PSDF (1) as

$$\begin{aligned} A(r\theta_d) &= \int_{-\infty}^{\infty} dz \frac{1}{(2\pi)^2} \int \int_{-\infty}^{\infty} P(\mathbf{m}) e^{im_x r\theta_d + im_z z} dm_x dm_z \\ &= \frac{2^{-\kappa+\frac{3}{2}}\sqrt{\pi}\varepsilon^2 a}{\Gamma(\kappa)} \left(\frac{r\theta_d}{a}\right)^{\kappa+1/2} K_{\kappa+1/2}\left(\frac{r\theta_d}{a}\right). \end{aligned} \tag{9}$$

The longitudinal integral A represents the correlation on a transverse direction. At a long travel distance from the source, the correlation of the wave field at two points spatially separated on a transverse axis rapidly decreases to zero with increasing lag distance [*Sato and Fehler*, 1998]. Then, the value of $A(0) - A(r\theta_d)$ at small transverse-distance $r\theta_d \ll a$ becomes important in the third term of equation (7). We may write the value as

$$A(0) - A(r\theta_d) \approx \varepsilon^2 a C(\kappa) \left(\frac{r\theta_d}{a}\right)^{p(\kappa)} \quad \text{for} \quad r\theta_d/a \ll 1. \tag{10}$$

Saito et al. [2002, 2003] numerically evaluated equation (10) by using equation (9) and estimated parameters $C(\kappa)$ and $p(\kappa)$ for given κ value at small transverse distances $10^{-4} < r\theta_d/a < 10^{-1}$. For example, $C = 0.56$ and $p = 1.19$ for the von Kármán–type random media of $\kappa = 0.1$, and $C = 1.50$ and $p = 1.99$ for $\kappa = 1.0$. The accuracy of the approximation (10) is graphically illustrated in Figure 4 of *Saito et al.* [2002].

[15] The TMCF Γ_2 can be decomposed into a product of ${}_0\Gamma_2$ and the wandering effect term, $\exp[-A(0)k_d^2 r/2]$. This term does not correspond to the broadening of the individual wave packet but shows the wandering effect from the statistical averaging of the travel time fluctuations of different rays at distance r [*Lee and Jokipii*, 1975]. Then the master equation for ${}_0\Gamma_2$ is given by

$$\frac{\partial}{\partial r}{}_0\Gamma_2 + i\frac{k_d}{2k_c^2}\frac{1}{r^2}\frac{\partial^2}{\partial\theta_d^2}{}_0\Gamma_2 + k_c^2[A(0) - A(r\theta_d)]{}_0\Gamma_2 = 0. \tag{11}$$

The ensemble average of the wave intensity at radial distance r and at lapse time t is

$$\begin{aligned} \left\langle |u(\mathbf{x},t)|^2 \right\rangle &= \frac{1}{(2\pi)^2}\frac{1}{r}\int_{-\infty}^{\infty} d\omega_c \int_{-\infty}^{\infty} d\omega_d \, e^{-\frac{A(0)r}{2V_0^2}\omega_d^2} \\ &\quad \cdot {}_0\Gamma_2(\theta_d = 0, r, \omega_d, \omega_c) e^{-i\omega_d(t - r/V_0)} \\ &= \frac{V_0}{2\pi}\int_{-\infty}^{\infty} d\omega_c \int_{-\infty}^{\infty} dt' w(\mathbf{x}, t - t') G_0(\mathbf{x}, t'; \omega_c), \end{aligned} \tag{12}$$

where the wandering effect in the time domain is given by

$$w(\mathbf{x},t) = \frac{1}{2\pi}\int_{-\infty}^{\infty} d\omega_d e^{-\frac{A(0)r}{2V_0^2}\omega_d^2} e^{-i\omega_d t} = \frac{V_0}{\sqrt{2\pi A(0) r}} e^{-\frac{V_0^2 t^2}{2A(0)r}}. \tag{13}$$

The wave intensity at distance r is given by a convolution integral of the wandering effect and function G_0 in the time domain. Function G_0 in equation (12) is given by the inverse Fourier transform of ${}_0\Gamma_2$ with respect to difference angular frequency ω_d,

$$\begin{aligned} G_0(\mathbf{x}, t; \omega_c) = \frac{1}{2\pi r V_0}\frac{1}{2\pi}\int_{-\infty}^{\infty} d\omega_d [2\pi_0\Gamma_2(\theta_d = 0, r, \omega_d, \omega_c)] \\ \cdot e^{-i\omega_d(t - r/V_0)}. \end{aligned} \tag{14}$$

Function G_0 must be real, that is, ${}_0\Gamma_2(\theta_d, r = 0, \omega_d, \omega_c) = {}_0\Gamma_2(\theta_d, r = 0, -\omega_d, \omega_c)^*$. We also note the causality $G_0 = 0$ for $t < r/V_0$. As the initial condition for the coherent isotropic radiation from a point source, we take ${}_0\Gamma_2$ to be nondimensional for a unit source radiation,

$$2\pi_0\Gamma_2(\theta_d, r = 0, \omega_d, \omega_c) = 1. \tag{15}$$

Then, G_0 has a dimension of spatial density and satisfies $G_0(\mathbf{x} \to 0, t; \omega_c) = \delta(t - r/V_0)/(2\pi V_0 r)$ as a limit. Function G_0 represents the MS envelope at central angular frequency ω_c for a unit source radiation. This is the mathematical definition of the Markov envelope. Numerically integrating equations (11) with (10) by using the Crank-Nicholson method [*Press et al.*, 1988], we obtain ${}_0\Gamma_2$ [see *Saito et al.*, 2002, 2003]. We plot the real and the imaginary parts of ${}_0\Gamma_2$ against difference angular frequency for von Kármán–type random media of $\kappa = 0.1$ in Figure 5a. By using the FFT of ${}_0\Gamma_2$ we can easily obtain the Markov envelope G_0. Figure 5b shows the time trace of the Markov envelope G_0, where the reduced time $t - r/V_0$ is normalized by the characteristic time,

$$t_M = \frac{C(\kappa)^{\frac{2}{p(\kappa)}}\varepsilon^{\frac{4}{p(\kappa)}} a}{2V_0}\left(\frac{a\omega_c}{V_0}\right)^{\frac{-2p(\kappa)+4}{p(\kappa)}}\left(\frac{r}{a}\right)^{\frac{p(\kappa)+2}{p(\kappa)}}. \tag{16}$$

The time width of envelope is well characterized by the characteristic time, whose frequency dependence is controlled by parameter $p(\kappa)$. Figure 6a shows plots of characteristic time t_M against travel distance at 2 Hz. The distance dependence of characteristic time is small when $\kappa = 1.0$ but large when $\kappa = 0.1$. Figure 6b shows plots of t_M against frequency at a distance of 200 km. When $\kappa = 0.1$, the characteristic time increases with increasing frequency and becomes larger than the travel time for frequencies higher than 7.5 Hz. However, it is small and nearly independent of frequency when $\kappa = 1.0$: $t_M = 3.82$ s at 2 Hz and 3.88 s at 10 Hz.

[16] Figure 7 schematically shows the scattering contribution of long-wavelength components and short-wavelength components of random inhomogeneity, where long-wave-

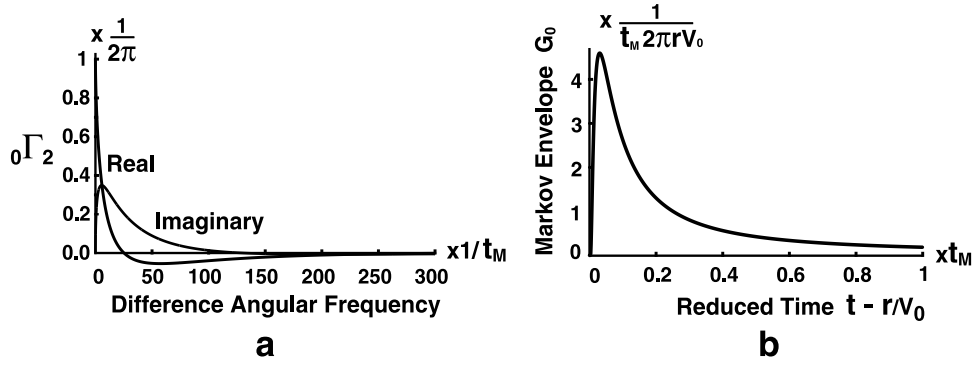

Figure 5. (a) Real and imaginary parts of ${}_0\Gamma_2$ as a function of difference frequency ω_d in von Kármán–type random media of $\kappa = 0.1$, where t_M is the characteristic time. (b) Markov envelope G_0 represents the mean square (MS) envelope for an impulsive isotropic source radiation in 2-D von Kármán–type random media of $\kappa = 0.1$.

length components cause the envelope broadening because of diffraction and forward scattering.

2.4. Comparison of Markov Envelopes With FD Envelopes

[17] In Figure 4, solid curves show MS envelopes in von Kármán–type random media directly simulated by using a convolution of the Markov envelope $G_0(\mathbf{x}, t; \omega_c)$, the wandering effect $w(\mathbf{x}, t)$ and the temporal change in the power of a 2 Hz Ricker wavelet source $W_R(t)$. We may say that solid curves well explain FD envelopes (shaded curves) around the peaks for both cases, $\kappa = 0.1$ and 1.0. The Markov approximation for the parabolic wave equation is able to predict at least the early wave envelopes quantitatively even for random media with rich short-wavelength spectra, because the early part is mainly composed of forward scattered waves. For the case of $\kappa = 1.0$, Markov envelopes and FD envelopes coincide well even in the coda; however, we find a departure of the Markov envelope from the FD envelope as lapse time increases at each receiver for the case of $\kappa = 0.1$. We may say that the coda part is mostly composed of waves that are scattered at large angles from short-wavelength inhomogeneities and they are correctly synthesized in FD envelopes; however, the large-angle scattering is completely neglected in the derivation of the Markov envelope.

[18] *Saito et al.* [2003] proposed to use the Markov envelope for the direct propagation term and to use the conventional radiative transfer theory for isotropic scattering to incorporate the effects of wide-angle scattering that leads to coda excitation. They have succeeded in simulating whole envelopes from onset to coda; however, their formulation contains some inconsistency: The propagator used in their radiative transfer equation is a delta function-type as $\delta(t - r/V_0)/(2\pi V_0 r)$, which does not represent diffraction effect due to long-wavelength spectra. In the following, extending their idea in a consistent manner, we propose a hybrid method for the envelope synthesis, in which we use the Markov envelope containing diffraction effect as a propagator in the radiative transfer integral equation.

3. Hybrid Simulation Based on the Radiative Transfer Theory

3.1. Momentum Transfer Scattering Coefficient

[19] Scattering power per unit area of a 2-D random media is characterized by the scattering coefficient, which can be estimated by using the Born approximation. The

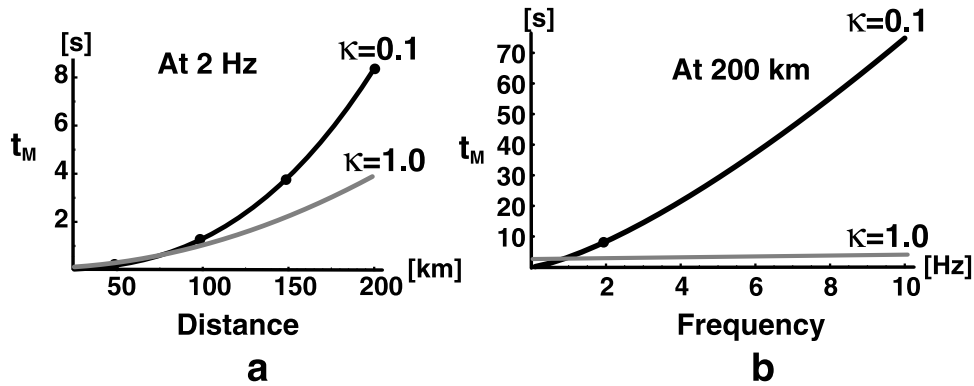

Figure 6. (a) Distance dependence of the characteristic time. (b) Frequency dependence of the characteristic time of the Markov approximation. Solid curves and shaded curves correspond to $\kappa = 0.1$ and $\kappa = 1.0$ for 2-D von Kármán–type random media of $V_0 = 4$ km/s, $\varepsilon = 5\%$, $a = 5$ km.

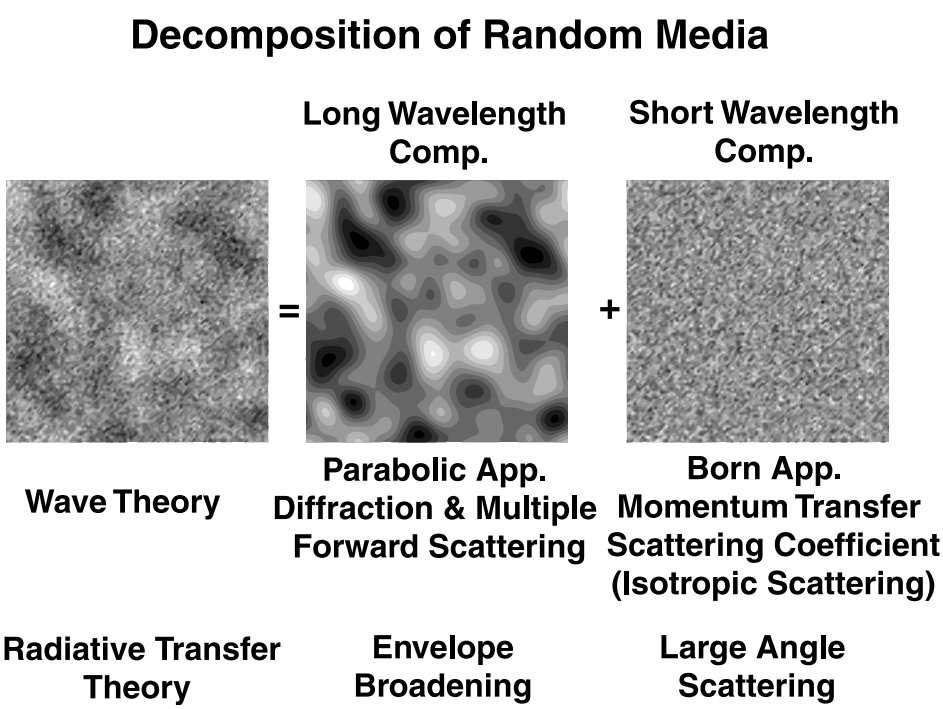

Figure 7. Schematic illustration of the decomposition of random media into long-wavelength components and short-wavelength components.

angular dependence of scattering coefficient $g(\psi)$ at scattering angle ψ for waves of angular frequency ω_c is controlled by the PSDF as [*Frankel and Clayton*, 1986; *Sato and Fehler*, 1998],

$$g(\psi;\omega_c) = \left(\frac{\omega_c}{V_0}\right)^3 P\left(2\frac{\omega_c}{V_0}\sin\frac{\psi}{2}\right). \tag{17}$$

In Figure 8a, a fine solid curve shows the angular dependence of $g(\psi)$ at 2 Hz in von Kármán–type random media with $V_0 = 4$ km/s, $\varepsilon = 5\%$, $a = 5$ km, and $\kappa = 0.1$. We find that the scattering pattern is far from isotropic. A large lobe in the forward direction represents strong forward scattering due to long-wavelength components of the random media.

[20] Even though scattering is nonisotropic, scattering process can be well described by isotropic scattering when multiple scattering is dominant. Deriving the diffusion equation from the transport equation for nonisotropic scattering, *Morse and Feshbach* [1953] introduced the momentum transfer scattering coefficient as the effective isotropic scattering coefficient,

$$\begin{aligned} g_m(\omega_c) &= \frac{1}{\pi}\int_0^{\pi}(1-\cos\psi)g(\psi;\omega_c)d\psi \\ &= \frac{1}{\pi}\int_0^{\pi} 2\sin^2\frac{\psi}{2}\left(\frac{\omega_c}{V_0}\right)^3 P\left(\frac{2\omega_c}{V_0}\sin\frac{\psi}{2}\right)d\psi. \end{aligned} \tag{18}$$

A reciprocal of g_m gives the transport mean free path. In the Monte Carlo simulation of energy particles in scattering media, *Gusev and Abubakirov* [1996] used g_m for characterizing the coda excitation. For the von Kármán–type random media of $V_0 = 4$ km/s, $\varepsilon = 5\%$, $a = 5$ km, and $\kappa = 0.1$, $g_m = 0.00273$ km^{-1} at 2 Hz. In Figure 8b, a bold solid curve shows a circle of radius g_m representing the effective isotropic scattering for 2 Hz waves, where a fine solid curve shows the scattering coefficient predicted by the Born approximation. Scattering at large angles is 3 orders of magnitude smaller than the forward scattering. A dashed curve shows the plot of the integrand of equation (18), $(1 - \cos\psi)g(\psi;\omega_c)$. The factor $(1 - \cos\psi)$ eliminates forward scattering, and the dashed curve is very close to the circle of g_m. This factor also works as a filter that eliminates

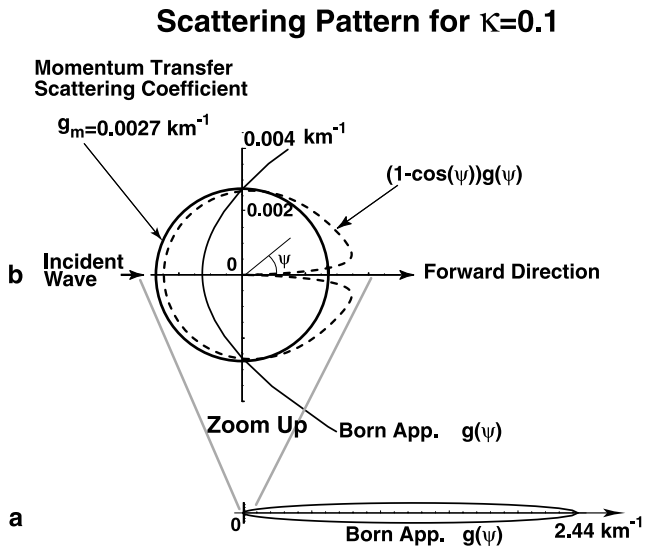

Figure 8. (a) Scattering pattern of 2 Hz waves in 2-D von Kármán–type random media of $V_0 = 4$ km/s, $\varepsilon = 5\%$, $a = 5$ km, and $\kappa = 0.1$. (b) Zoom up of the scattering pattern.

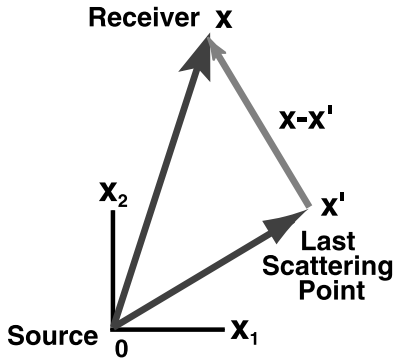

Figure 9. Configuration of a source, a receiver, and a last scattering point used in the radiative transfer integral equation.

small-wave number components of the spectra (long-wavelength spectra) of the random media. That is, the momentum transfer scattering coefficient represents the effective isotropic scattering, which is the average contribution of large-angle scattering due to short-wavelength spectra of random media as conceptually illustrated in Figure 7.

3.2. Radiative Transfer Equation

[21] We develop an envelope synthesis on the basis of the radiative transfer theory [*Shang and Gao*, 1988; *Zeng et al.*, 1991], where the energy density in the radiative transfer equation represents the MS wave amplitude at a given angular frequency. We here propose to use the Markov envelope G_0 as a propagator in the radiative transfer integral equation. The Markov envelope reliably represents causality and envelope broadening caused by scattering due to the long-wavelength spectra of random media. We use the momentum transfer scattering coefficient g_m, which reliably models the large-angle scattering caused by the short-wavelength spectra of random media, as the effective isotropic scattering coefficient in the radiative transfer equation. The objective is to derive the space-time distribution of energy density $G(\mathbf{x}, t; \omega_c)$ for an isotropic unit source radiation. Figure 9 shows the geometry used for the description of radiative transfer integral equation. The radiative transfer equation for a unit isotropic source radiation in a 2-D medium with no intrinsic absorption is written by using the convolution integral equation as

$$G(\mathbf{x}, t; \omega_c) = G_0(\mathbf{x}, t; \omega_c) e^{-\mu g_m V_0 t} + V_0 g_m \int_{-\infty}^{\infty} \int_{-\infty}^{\infty} \int_{-\infty}^{\infty} \cdot G_0(\mathbf{x} - \mathbf{x}', t - t'; \omega_c) \cdot e^{-\mu g_m V_0 (t - t')} G(\mathbf{x}', t'; \omega_c) dt' d\mathbf{x}', \quad (19)$$

where the exponential term $\exp[-\mu g_m V_0 t]$ representing scattering loss is introduced to conserve the total energy. The conservation of total energy $\int\int_{-\infty}^{\infty} G(\mathbf{x}, t; \omega_c) d\mathbf{x} = 1$ gives the value of parameter μ. We may call $G(\mathbf{x}, t; \omega_c)$ the Green function for the hybrid synthesis and the time trace as the hybrid envelope. We note that the scattering loss term $\exp[-g_m V_0 t]$ was introduced for the delta function propagator $\delta(t - r/V_0)/(2\pi V_0 r)$ in the conventional radiative transfer theory [*Shang and Gao*, 1988].

[22] As schematically illustrated in Figure 10a, the delta function propagator describing causality with a constant velocity is used in the conventional radiative transfer theory for isotropic scattering [*Shang and Gao*, 1988; *Zeng et al.*, 1991; *Yoshimoto*, 2000] and/or nonisotropic scattering [*Sato*, 1994; *Hoshiba*, 1995; *Gusev and Abubakirov*, 1996]. The Born approximation predicts large forward scattering due to the long-wavelength spectra of random media. The concept of the new hybrid synthesis is schematically shown on Figure 10b, where we assume isotropic scattering due to short-wavelength components but include

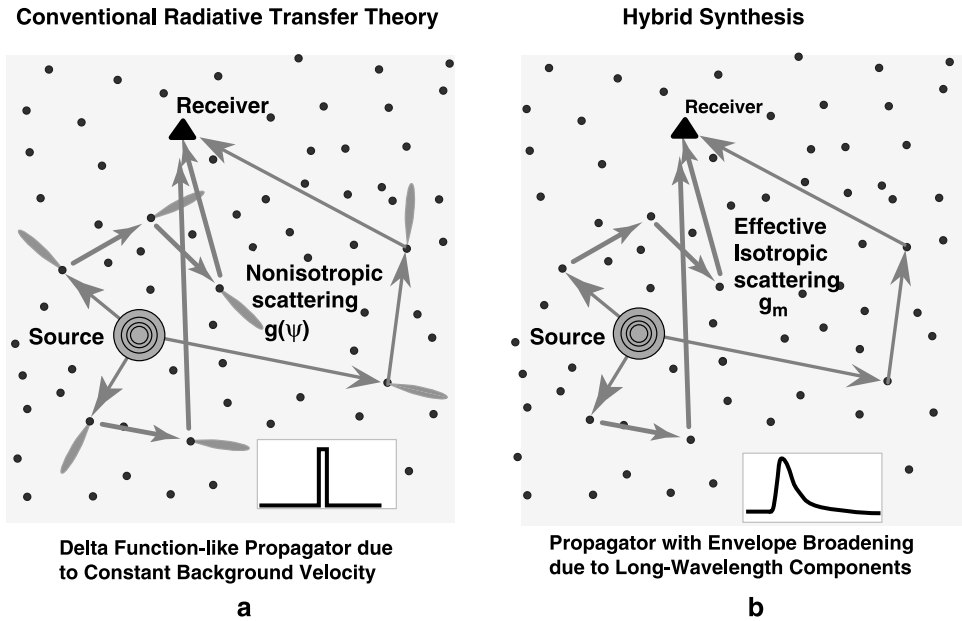

Figure 10. Concept of the (a) conventional radiative transfer theory and (b) hybrid synthesis.

Table 1. Mutual Relations Between Three Approaches

	Wave Theory	Markov Approximation	Hybrid Synthesis
Field	wave field $u(\mathbf{x}, t) = \frac{1}{2\pi\sqrt{r}}\int U e^{i(kr-\omega t)}d\omega$	two-frequency mutual coherence function $\Gamma_2 = \langle UU^* \rangle$	energy density $G(\mathbf{x}, t; \omega_c)$
Medium inhomogeneities	wave velocity $V(\mathbf{x}) = V_0\{1 + \xi(\mathbf{x})\}$	longitudinal integral of ACF $A(r\theta_d) = \int_{-\infty}^{\infty} R(r\theta_d, z)dz$	broadening coefficient $g_b(\omega_c) = \frac{C(\kappa)}{2^{\frac{p(\kappa)}{2}}}\frac{\varepsilon^2}{a}\left(\frac{a\omega_c}{V_0}\right)^{2-p(\kappa)}$
	ensemble of random media $\{\xi(\mathbf{x})\}$	$A(0) - A(r\theta_d) \approx \varepsilon^2 a C(\kappa)\left(\frac{r\theta_d}{a}\right)^{p(\kappa)}$ for $\left\|\frac{r\theta_d}{a}\right\| \ll 1$	
von Kármán–type random media	ACF $R(\mathbf{x}) \equiv \langle \xi(\mathbf{x} + \mathbf{x}')\xi(\mathbf{x}') \rangle$		momentum transfer scattering coefficient $g_m(\omega_c) = \frac{1}{\pi}\int_0^{\pi}(1 - \cos\psi)g(\psi; \omega_c)d$
	PSDF $P(\mathbf{m}) = \int\int_{-\infty}^{\infty} R(\mathbf{x})e^{-i\mathbf{m}\mathbf{x}}d\mathbf{x} = \frac{4\pi\varepsilon^2 a^2\kappa}{(1+a^2m^2)^{\kappa+1}}$		scattering coefficient (Born approximation) $g(\psi; \omega_c) = \left(\frac{\omega_c}{V_0}\right)^3 P\left(\frac{2\omega_c}{V_0}\sin\frac{\psi}{2}\right)$

envelope broadening due to long-wavelength components during propagation between isotropic scatterers.

3.3. Scale Parameter Characterizing Envelope Broadening due to Diffraction

[23] Introducing a new parameter g_b having a dimension of the reciprocal of length, we can represent the characteristic time for envelope broadening due to diffraction as

$$t_M = \frac{(g_b\, r)^{1+\frac{2}{p(\kappa)}}}{g_b V_0}, \tag{20}$$

where

$$g_b(\omega_c) = \frac{C(\kappa)}{2^{\frac{p(\kappa)}{2}}}\frac{\varepsilon^2}{a}\left(\frac{a\omega_c}{V_0}\right)^{2-p(\kappa)}. \tag{21}$$

We call new parameter g_b the broadening coefficient. For the von Kármán–type random media of V_0 = 4 km/s, ε = 5%, a = 5 km, and κ = 0.1, g_b = 0.0017254 km^{-1} at 2 Hz.

[24] We note that there are two scales g_b and g_m, which characterize the diffraction effect due to long-wavelength components and the average scattering contribution due to short-wavelength components. Table 1 shows mutual relations between the wave theory, the Markov approximation, and the hybrid synthesis.

3.4. Radiative Transfer Equation in Nondimensional Form

[25] We normalize all the parameters for describing the scattering process by using broadening coefficient g_b and the average velocity V_0 as

$$\begin{gathered} \bar{r} = g_b r, \bar{t} = g_b V_0 t, \bar{\omega}_d = \frac{\omega_d}{g_b V_0}, \bar{t}_M = g_b V_0 t_M = \bar{r}^{1+\frac{2}{p(\kappa)}}, \\ \bar{g}_m = \frac{g_m}{g_b}, g_b^2\bar{G}_0 = G_0, g_b^2\bar{G} = G. \end{gathered} \tag{22}$$

For example, a distance of 200 km is 0.345 in normalized distance and a time of 50 s is 0.345 in normalized time. For the von Kármán–type random media of V_0 = 4 km/s, ε = 5%, a = 5 km, and κ = 0.1, both g_b and g_b increase with increasing frequency as shown in Figure 11a; however, the ratio $\bar{g}_m = g_m/g_b$ = 1.58 at 2 Hz and converges to a finite value 1.63 with increasing frequency as shown in Figure 11b.

[26] Then, the Markov propagator equation (14) in nondimensional form is

$$\bar{G}_0(\bar{\mathbf{x}}, \bar{t}, \bar{\omega}_c) = \frac{1}{2\pi}\int_{-\infty}^{\infty} d\bar{\omega}_d e^{-i\bar{\omega}_d\bar{t}}\left[\frac{1}{2\pi\bar{r}}e^{i\bar{\omega}_d\bar{r}}2\pi_0\Gamma_2\left(\bar{r}^{1+\frac{2}{p}}\bar{\omega}_d\right)\right]. \tag{23}$$

The radiative transfer equation in nondimensional form is written as

$$\begin{aligned} \bar{G}(\bar{\mathbf{x}}, \bar{t}, \bar{\omega}_c) &= \bar{G}_0(\bar{\mathbf{x}}, \bar{t}, \bar{\omega}_c)e^{-\mu\bar{g}_m\bar{t}} \\ &\quad + \bar{g}_m\int_{-\infty}^{\infty}\int_{-\infty}^{\infty}\int_{-\infty}^{\infty}\bar{G}_0\left(\bar{\mathbf{x}} - \bar{\mathbf{x}}', \bar{t} - \bar{t}', \bar{\omega}_c\right)e^{-\mu\bar{g}_m(\bar{t}-\bar{t}')} \\ &\quad \cdot \bar{G}\left(\bar{\mathbf{x}}', \bar{t}', \bar{\omega}_c\right)\cdot d\bar{t}'d\bar{\mathbf{x}}'. \end{aligned} \tag{24}$$

As shown in Figure 5b, we have already obtained the Markov envelope in space and time. Substituting the Fourier transform of $\bar{G}_0(\bar{\mathbf{x}}, \bar{t}, \bar{\omega}_c)e^{-\mu\bar{g}_m\bar{t}}$ in space and time into the Fourier transform of equation (24), we can easily solve the radiative transfer integral equation. By using the

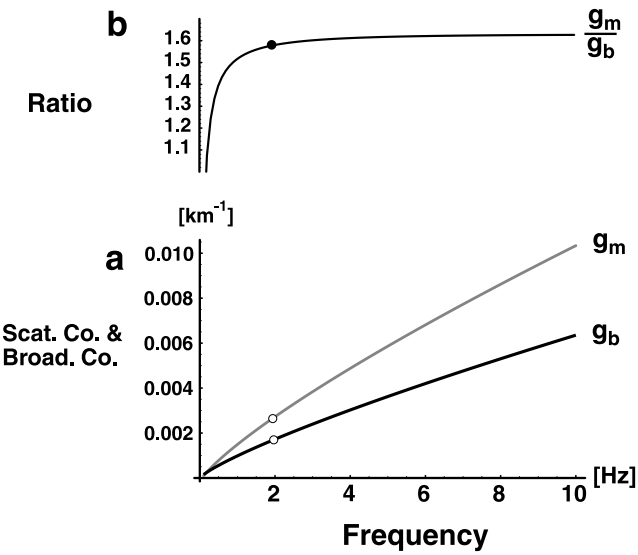

Figure 11. (a) Frequency dependence of the broadening coefficient (solid) and the momentum transfer scattering coefficient (shaded) for 2-D von Kármán–type random media of V_0 = 4 km/s, ε = 5%, a = 5 km, and κ = 0.1. (b) Frequency dependence of the ratio.

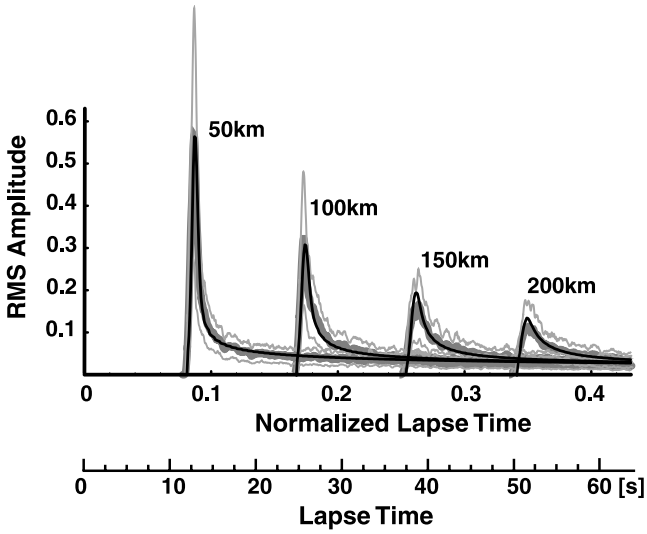

Figure 12. Root-mean-square (RMS) envelopes of waves for a 2 Hz Ricker wavelet source radiation in 2-D von Kármán–type random media of V_0 = 4 km/s, ε = 5%, a = 5 km, and κ = 0.1. Each numeral shows the distance from the source. Solid curves and thick shaded curves show RMS envelopes based on the hybrid synthesis and those by FD simulations, respectively. Fine shaded curves show ±1 standard deviation of FD envelopes.

inverse Fourier transform, we numerically obtain $\overline{G}(\overline{\mathbf{x}}, \overline{t}; \omega_c)$ in space and time.

[27] From the requirement of total energy conservation, we numerically evaluate the value of μ for a given lapse time range. At 2 Hz, in the case of von Kármán–type random media of V_0 = 4 km/s, ε = 5%, a = 5 km, and κ = 0.1, we have to take μ = 0.50 in order to satisfy the total energy conservation with accuracy of 99% for a normalized lapse time interval from 0.02 to 0.4. In Figure 12, shaded curves show RMS FD envelopes at four receivers with a 50 km separation for the 2 Hz Ricker-wavelet isotropic source radiation, where the thick shaded curve is the mean RMS envelope and the fine shaded curves are ±1 standard deviation curves at each distance. Solid curves show RMS envelopes synthesized by the new hybrid method. In the synthesis of MS envelopes, we used the convolution in time of the hybrid envelope $G(\mathbf{x}, t; \omega_c)$, the wandering effect $w(\mathbf{x}, t)$ and the temporal change in the power of 2 Hz Ricker wavelet source $W_R(t)$. We label the abscissa to show both seconds and normalized lapse time. At all travel distances, the hybrid envelopes are in good agreement with the FD envelopes from the onset through coda.

[28] Figure 13 zooms up RMS envelopes at a distance of 100 km from the source. We can see that the fit of the hybrid envelope (thick solid curve) to the FD envelope (shaded curve) is excellent around the peak arrival and through the coda; however, the hybrid envelope is a little smaller than the FD envelope in a transient stage around normalized lapse time of 0.2. We also plot the contribution of the Markov envelope with scattering loss by a fine solid curve and the large-angle scattering term by a fine dashed curve separately. The Markov envelope dominates around the peak arrival and the effective isotropic scattering representing large-angle scattering mainly contributes to the coda. The small disagreement in the transient stage is due to the use of effective isotropic scattering earlier than the multiple scattering regime since the momentum transfer scattering coefficient well characterizes effective scattering process only in the multiple scattering regime. Figure 13 shows a good coincidence between FD envelope and hybrid envelope as lapse time increases. *Gusev and Abubakirov* [1996] confirmed the validity of the use of the momentum transfer scattering coefficient at large lapse time based on the Monte Carlo method.

4. Summary and Discussions

[29] As a mathematical basis for the study of high-frequency seismic wave propagation through the heterogeneous lithosphere, we developed a method to synthesize scalar wave envelopes for 2-D media containing random velocity inhomogeneities, particularly those containing structure that is smaller than the propagation wavelength. The main framework is the radiative transfer theory for the isotropic scattering process. Instead of the delta function type propagator, the envelope derived from the Markov approximation is used as a propagator in the radiative transfer integral equation. That propagator reflects the envelope broadening effect due to diffraction caused by the long-wavelength spectra of random velocity inhomogeneity. In the radiative transfer integral equation, large-angle scattering caused by the short-wavelength inhomogeneity can be effectively modeled by using the isotropic scattering process, where the momentum transfer scattering coefficient is used as the effective isotropic scattering coefficient. For the case of a 2 Hz Ricker wavelet isotropic source radiation in 2-D von Kármán–type random media of V_0 = 4 km/s, ε = 5%, a = 5 km, and κ = 0.1, we found an excellent agreement between the envelopes calculated by using the new hybrid method and the FD envelopes. In random media having poor short-wavelength spectra, for example, von Kármán–type random media of κ = 1.0, the simple use of the Markov approximation

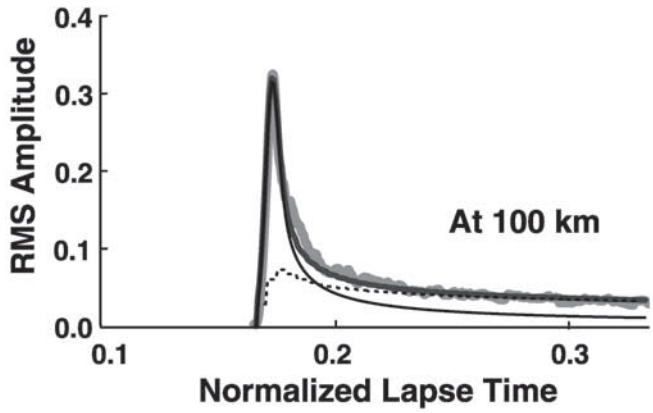

Figure 13. Thick solid curve shows the RMS envelope of waves at a distance of 100 km predicted by the hybrid synthesis for a 2 Hz Ricker wavelet source radiation in 2-D von Kármán–type random media of V_0 = 4 km/s, ε = 5%, a = 5 km, and κ = 0.1. A fine solid curve and a fine dashed curve show the Markov envelope with scattering loss and the contribution of large-angle scattering, respectively. A shaded curve shows the FD envelope.

is enough for simulating envelopes from the onset to coda. Thus we have now succeeded in directly simulating envelopes in both extreme cases, $\kappa = 0.1$ and $\kappa = 1.0$.

[30] We made a comparison only for the case of 2 Hz waves since the FD simulations take considerable time to calculate [see *Fehler et al.*, 2000]. We may say that the model is applicable when the fractional fluctuation is small. We expect that the hybrid method would be successful for higher-frequency bands because of self-similarity of the media spectra; however, as noted, the characteristic time of the Markov approximation increases to the order of the travel time and the transport mean free path becomes shorter with increasing frequencies. It suggests that the applicable range of the proposed synthesis for higher frequencies should be carefully examined by comparison with numerical simulations. It is the key to get the Markov envelope that is used as a propagator in the radiative transfer integral equation; however, we have practically succeeded in getting Markov envelopes in limited types of spectra as Gaussian and von Kármán–type only. It is necessary for us to examine the applicability of the hybrid method to random media having different spectral types. We should be more cautious in using the Born approximation in high frequencies even if large scattering in the forward direction is neglected in the calculation of momentum transfer scattering coefficient. The validity of momentum transfer scattering coefficient as an effective isotropic scattering coefficient should be practically examined as noted by *Saito et al.* [2003]. Furthermore, it will be necessary to extend the hybrid synthesis to the 3-D case and examine the validity from a comparison with envelopes of waves numerically synthesized by the finite difference simulation.

[31] This paper gives a possible approach for the direct derivation of wave envelopes in random media. If we carefully examine the frequency dependence of envelopes more precisely in relation with the spectral structure of random media, we will be able to construct a mathematical basis of the inversion scheme for estimating the spectral structure of random media. An extension of scalar wave theory to elastic wave theory is highly desired. Such an approach can be considered as one of the practical methods to interpret high-frequency seismograms.

[32] **Acknowledgments.** We are grateful to A.E., Justin Revenaugh and two anonymous reviewers for their helpful comments. H. S. and T. S. are partially supported by the Japan-Germany research cooperative program of JSPS, Grant-in-Aid for JSPS Fellows (10530), and a grant from NISA, METI, Japan.

References

Aki, K. (1980), Attenuation of shear-waves in the lithosphere for frequencies from 0.05 to 25 Hz, *Phys. Earth Planet. Inter.*, *21*, 50–60.

Atkinson, G. M. (1993), Notes on ground motion parameters for eastern North America: Duration and H/V ratio, *Bull. Seismol. Soc. Am.*, *83*, 587–596.

Fehler, M., H. Sato, and L.-J. Huang (2000), Envelope broadening of outgoing waves in 2-D random media: A comparison between the Markov approximation and numerical simulations, *Bull. Seismol. Soc. Am.*, *90*, 914–928.

Frankel, A., and R. W. Clayton (1986), Finite difference simulations of seismic scattering: Implications for the propagation of short-period seismic waves in the crust and models of crustal heterogeneity, *J. Geophys. Res.*, *91*, 6465–6489.

Fukushima, Y., O. Nishizawa, H. Sato, and M. Ohtake (2003), Laboratory study on scattering characteristics of shear waves in rock samples, *Bull. Seismol. Soc. Am.*, *93*, 253–263.

Goff, J. A., and K. Holliger (1999), Nature and origin of upper crustal seismic velocity fluctuations and associated scaling properties: Combined stochastic analyses of KTB velocity and lithology logs, *J. Geophys. Res.*, *104*, 13,169–13,182.

Gusev, A. A., and I. R. Abubakirov (1996), Simulated envelopes of non-isotropically scattered body waves as compared to observed ones: Another manifestation of fractal heterogeneity, *Geophys. J. Int.*, *127*, 49–60.

Higdon, R. L. (1991), Absorbing boundary conditions for elastic waves, *Geophysics*, *56*, 231–241.

Holberg, O. (1987), Computational aspects of the choice of operator and sampling interval for numerical differentiation in large-scale simulation of wave phenomena, *Geophys. Prospect.*, *35*, 629–655.

Hoshiba, M. (1995), Estimation of nonisotropic scattering in western Japan using coda wave envelopes: Application of a multiple nonisotropic scattering model, *J. Geophys. Res.*, *100*, 645–657.

Ishimaru, A. (1978), *Wave Propagation and Scattering in Random Media*, vols. 1 and 2, Academic, San Diego, Calif.

Kravstov, Y. A. (1992), Propagation of electromagnetic waves through a turbulent atmosphere, *Rep. Prog. Phys.*, *55*, 39–112.

Lee, L. C., and J. R. Jokipii (1975), Strong scintillations in astrophysics: II. A theory of temporal broadening of pulses, *Astrophys. J.*, *201*, 532–543.

Liu, Y. B., and R. S. Wu (1994), A comparison between phase screen, finite difference, and eigenfunction expansion calculations for scalar waves in inhomogeneous media, *Bull. Seismol. Soc. Am.*, *84*, 1154–1168.

Morse, P. M., and H. Feshbach (1953), *Methods of Theoretical Physics*, McGraw-Hill, New York.

Obara, K., and H. Sato (1995), Regional differences of random inhomogeneities around the volcanic front in the Kanto-Tokai area, Japan, revealed from the broadening of *S* wave seismogram envelopes, *J. Geophys. Res.*, *100*, 2103–2121.

Press, W. H., S. A. Terkolsky, W. T. Vetterling, and B. P. Flannery (1988), *Numerical Recipes in C*, Cambridge Univ. Press, New York.

Saito, T., H. Sato, and M. Ohtake (2002), Envelope broadening of spherically outgoing waves in three-dimensional random media having power law spectra, *J. Geophys. Res.*, *107*(B5), 2089, doi:10.1029/2001JB000264.

Saito, T., H. Sato, M. Fehler, and M. Ohtake (2003), Simulating the envelope of scalar waves in 2D random media having power-law spectra of velocity fluctuation, *Bull. Seismol. Soc. Am.*, *93*, 240–252.

Sato, H. (1984), Attenuation and envelope formation of three-component seismograms of small local earthquakes in randomly inhomogeneous lithosphere, *J. Geophys. Res.*, *89*, 1221–1241.

Sato, H. (1989), Broadening of seismogram envelopes in the randomly inhomogeneous lithosphere based on the parabolic approximation: Southeastern Honshu, Japan, *J. Geophys. Res.*, *94*, 17,735–17,747.

Sato, H. (1994), Formulation of the multiple non-isotropic scattering process in 2-D space on the basis of energy transport theory, *Geophys. J. Int.*, *117*, 727–732.

Sato, H., and M. Fehler (1998), *Seismic Wave Propagation and Scattering in the Heterogeneous Earth*, Springer-Verlag, New York.

Sato, H., M. Fehler, and R. S. Wu (2002), Scattering and attenuation of seismic waves in the lithosphere, in *International Handbook of Earthquake and Engineering Seismology*, edited by W. H. K. Lee et al., chap. 13, pp. 195–208, Academic, San Diego, Calif.

Scherbaum, F., and H. Sato (1991), Inversion of full seismogram envelopes based on the parabolic approximation: Estimation of randomness and attenuation in southeast Honshu, Japan, *J. Geophys. Res.*, *96*, 2223–2232.

Shang, T., and L. Gao (1988), Transportation theory of multiple scattering and its application to seismic coda waves of impulsive source, *Sci. Sin., Ser. B*, Engl. Ed., *31*, 1503–1514.

Shiomi, K., H. Sato, and M. Ohtake (1997), Broad-band power-law spectra of well-log data in Japan, *Geophys. J. Int.*, *130*, 57–64.

Shishov, V. L. (1974), Effect of refraction on scintillation characteristics and average pulsars, *Sov. Astron.*, Engl. Transl., *17*, 598–602.

Tatarskii, V. I. (1971), *The Effects of the Turbulent Atmosphere on Wave Propagation*, Isr. Program for Sci. Transl., Jerusalem.

Wu, R. S., and K. Aki (1985), The fractal nature of the inhomogeneities in the lithosphere evidenced from seismic wave scattering, *Pure Appl. Geophys.*, *123*, 805–818.

Yoshimoto, K. (2000), Monte Carlo simulation of seismogram envelopes in scattering media, *J. Geophys. Res.*, *105*, 6153–6161.

Zeng, Y., F. Su, and K. Aki (1991), Scattering wave energy propagation in a random isotropic scattering medium: 1. Theory, *J. Geophys. Res.*, *96*, 607–619.

M. Fehler, Los Alamos National Laboratory, Los Alamos, NM 87545, USA.

T. Saito and H. Sato, Department of Geophysics, Tohoku University, Sendai-shi, Miyagi-ken 980-8578, Japan. (sato@zisin.geophys.tohoku.ac.jp)